

Supporting Information

Linking Nanoscale Chemical Changes to Bulk Material Properties in IEPM Polymer Composites Subject to Impact Dynamics

Thomas Attard¹, Li He¹*

¹University of Alabama at Birmingham, Department of Civil, Construction, and
Environmental Engineering, Birmingham, AL 35294

*Corresponding author.
Phone: +1-702-439-2417
E-mail: thoma1@uab.edu

MATERIALS AND METHODS

IEPM Synthesis. This study focuses on a time-point to apply polyurea to curing epoxy (t_c), utilizing fast-curing non-catalytic two-part aliphatic polyurea (FSS42D Part A: Isophorone Diisocyanate (IPDI) reacts with Polyoxypropylene Diamine; FSS42D Part B (resin): Diamine) - purchased from Versaflex Incorporated, USA - and a low-viscosity epoxy (544 cps) - Bisphenol A Diglycidyl ether (*DGEBA*) epoxy resin (LAM-125 resin) and LAM-226 polyamine hardener - purchased from Pro-Set Inc., USA. In the ballistics testing, we examined two-component aliphatic polyurea and aromatic polyurea, where Part A of the latter was comprised of Methylene Diisocyanate (*MDI*) and Polyether Polyol. Epoxy resin and NH_2 -based hardener were mixed by a volume ratio of 3:1 at room temperature. Effects of epoxy viscosity on *IEPM* were studied by synthesizing *IEPM* using $t_c=0.5$ h and $t_c=2.5$ h with a higher-viscosity epoxy (1,367 cps): LAM-135 resin and 226 hardener. Various combinations of potential chemical reactions are shown in Table S1. Figure S1 depicts a suggested reaction based on the high reaction rate of Reaction 2 and because we found single nanoscale locations to consistently feature both polyurea and epoxy peaks. In the construction of *C-IEPM-b- t_c* panels, carbon fiber sheets (2x2 Twill architecture, 5.78 oz / yd², 550 ksi tensile strength, 0.33 mm fiber thickness) were purchased from ACP Composites, Inc., USA.

Table S1. Possible *IEPM* chemical reactions: curing epoxy / polyurea (pre-polymerized)

Reaction number	Polyurea component	Epoxy component	Reactions being tested	Preliminary Observations	Discussion/ Explanation
1	Part A (diisocyanate)	Resin (DGEBA)	-NCO + epoxide -NCO + -OH	No reaction	N/A
2	Part A (diisocyanate)	Hardener (polyamine)	-NCO + -NH ₂ (epoxy hardener)	Solidifies in seconds after mixing	-NCO + -NH ₂ rapid reaction
3	Part B (polyamine)	Resin (DGEBA)	Epoxide + -NH ₂ (polyurea part B)	Mixed, no reaction after 24 hours	Additives in epoxy part B accelerate the reaction of epoxide + NH ₂

4	Part A (diisocyanate)	Curing epoxy (3:1 ratio resin: hardener)	-NCO + - NH ₂ (epoxy hardener) at the interface	-NCO on the top, still liquid after 24 hours	Possible -NCO + NH ₂ / - NCO + epoxide reaction at the interface, but no reaction in top layer -NCO
5	Part A (diisocyanate)	Curing epoxy (2:1 ratio resin: hardener)	-NCO + - NH ₂ (epoxy hardener) at the interface	-NCO on the top, still liquid after 24 hours	Possible -NCO + NH ₂ / - NCO + epoxide reaction at the interface, but no reaction in top layer -NCO

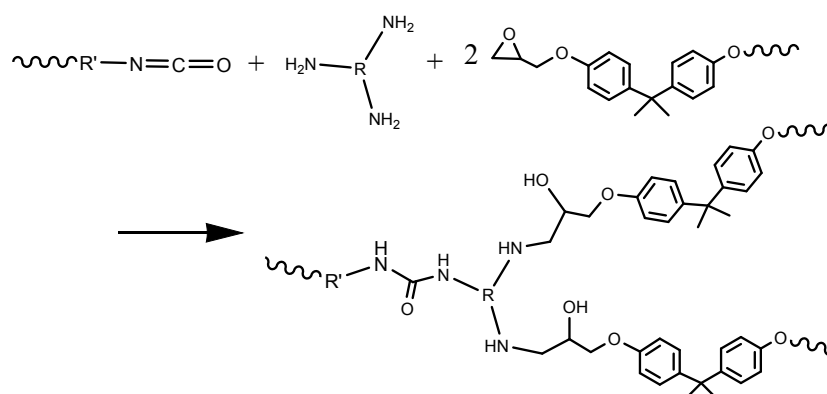


Figure S1. Schematic of suggested reaction, where formation of chemical bonding within the *IEPM* (interface) consists of the three-part reaction: (epoxide) + (amine epoxy hardener) + (isocyanate)

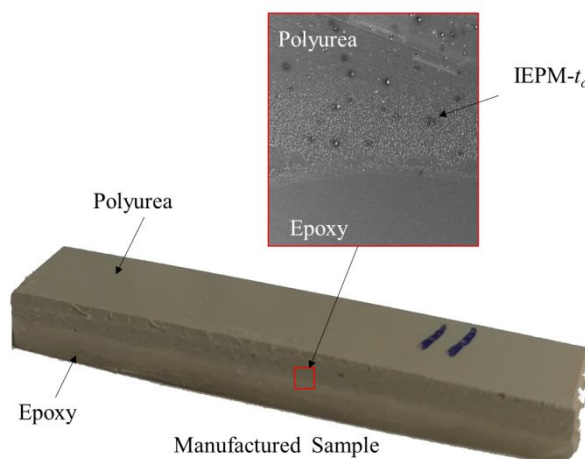


Figure S2. Manufactured 0-IEPM- t_c sample and SEM image of 0-IEPM- t_c

IEPM is a reaction between epoxy and pre-polymerized fast-curing polyurea. Multiple elapsed curing times of epoxy resin (t_c) were selected as time-points (0 h, 0.5 h, 1 h, 1.5 h, 2.5 h, 3.5 h, and 24 h) to spray polyurea on curing epoxy. Figure S2 shows one of the manufactured samples and its SEM image of IEPM. For C-IEPM- t_c fabrication, carbon (C) fiber sheets were immersed in epoxy mixture. For 0-IEPM- t_c

fabrication (“x” is 0), the just-mixed epoxy mixture ($t_c=0$), signifying commencing of curing, was poured onto a substrate as the bottom layer. Polyurea was then applied onto curing epoxy at 70 °C using a polyurea spray machine (Reactor E-10, Graco Inc., USA) with a high-pressure spray gun (at 1000 psi and 70 °C). At the conclusion of the spray process, specimens remained in a curing state for 24 h before being cut (via electric table saw) and tested under mechanical loading (*DMA* and up to .44 magnum ballistics testing). The specimens were named in accordance to type of fiber (“x”) that was used and t_c , see Table S2. Specimens that utilized LAM 135 / 226 were designated as C-*IEPM*-0.5v and C-*IEPM*-2.5v. Specimens that were constructed as ballistics panels were designated as x-*IEPM*-b- t_c (b = ballistics) and were manufactured as follows: Using two wood-constructed frames as support-structures, two groups of five fiber sheets were individually epoxied. The last layer was sprayed with polyurea, engendering “inner” *IEPM* reaction; the back-side of the first layer was not sprayed. Aromatic and aliphatic polyurea cures after approximately 10 sec and 90 sec, per manufacturer recommendation. Five additional fiber layers, intermittently epoxied, were applied to the two cured polyurea surfaces. The last layer was sprayed with polyurea, engendering “outer” *IEPM* reaction at approximately $t_c = 2.5$ h. The two “inner-outer” half-panels were epoxied together, back-fiber-side to back-fiber-side. The four-layer panel was removed from its adjoined wood frame.

Table S2. Specimen names and corresponding parameters

Specimen Name	t_c (hr)	IEPM Width (μm)	Fiber Type (‘x’)
0-IEPM-0	0	50	0
0-IEPM-0.5	0.5	30	0
0-IEPM-1	1	10	0
0-IEPM-1.5	1.5	< 2	0
0-IEPM-2.5	2.5	< 2	0
0-IEPM-3.5	3.5	< 2	0
0-IEPM-24	24	0	0
C-IEPM-0.5V	0.5	< 10	C (Carbon), 2-layer
C-IEPM-2.5V	2.5	< 2	C(2-layer)
C-IEPM-0	0		C(2-layer)

C-IEPM-0.5	0.5	C(2-layer)
C-IEPM-1	1	C(2-layer)
C-IEPM-1.5	1.5	C(2-layer)
C-IEPM-2.5	2.5	C(2-layer)
C-IEPM-3.5	3.5	C(2-layer)
C-IEPM-24	24	C(2-layer)
C-IEPM-b- t_c	t_c varies	C(4-layer/2-layer)

Characterization. Scanning electron microscopy (*SEM*), (Zeiss, USA), was implemented to observe the fracture surfaces of x-*HMC* / *IEPM*- t_c cross sections to study the thickness and morphology of interface. Atomic force microscope (*AFM*) and nano-Infrared Spectroscopy (nano-IR) were carried out to study the morphology and chemical composition of the interface area respectively (Nano-IR2, Anasys Instruments, USA). All *AFM* and nano-IR measurements were carried out in contact mode using commercially available Au coated Si cantilevers with a nominal resonance frequency of 13 ± 4 kHz, spring constant of 0.07-0.04 N/m, and 50 nm radius of curvature. Prior to nano-IR characterization, the specimens were trimmed and cut to a dimension of 1mm by 1mm by 200 nm using Microtome (Zeiss, USA).

Mechanical properties of six x-*HMC*/ *IEPM*- t_c specimens, see Table S3, were measured using Dynamic Mechanical Analyzer (*DMA*). Bar specimens were cut to size 30 mm by 7 mm and tested in single cantilever mode at room temperature using a RSA-G2 Solids Analyzer instrument (USA). In order to identify *IEPM* properties, we effectively isolated *IEPM* in each 0-*IEPM*- t_c specimen via multi-layered parallel Generalized Maxwell Model (epoxy, polyurea, and *IEPM*). Using measured DMA results for pure polyurea and pure epoxy, shown in Figure S3, we normalized test results according to a Thickness Factor, m , using each sample's thickness and the maximum thickness of the group of six samples, to account for experimental variation¹.

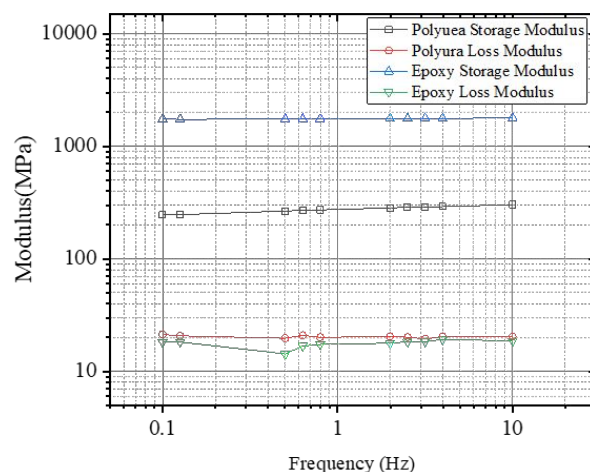


Figure S3. DMA results of pure polyurea and pure epoxy, Set-up of Test Program B, including wood-constructed support structure, chronograph, and $C-IEPM-b-t_c$ test panel

Microtoming reveals Shifting of nano-IR Spectra Peaks. The 1090 cm^{-1} absorption peak shifts to 1115 cm^{-1} in $0-IEPM-2.5$, see Figure 2(i), which could be explained by weak hydrogen bonding with absorbed water during the microtome process. However, since nano-IR point spectra were not collected on the “black holes” in Figure 2(h), this does not appear to be the case. Furthermore, the 1090 cm^{-1} peak was not observed to shift in $0-IEPM-0$ Figures 1(d) and 1(e), $0-IEPM-0.5$ Figure 2(c), and $0-IEPM-1$, see Figure 2(f).

Non-Negative Matrix Factorization (NMF). A line of 100 points was selected to perform nano-IR spectral analyses from pure-epoxy region, across the $IEPM$, to pure-polyurea region for all $x-IEPM-t_c$ specimens. We rearranged the nano-IR spectra of all points per $IEPM$ to form a nano-IR spectra matrix V and used Non-Negative Matrix Factorization (NMF) to de-convolute the spectra using matrix W (wave number spectra) and intensity matrix H by $V = W \times H$. All three matrices have no negative elements. Each vector in W is a de-convoluted vector of a single IR spectrum along the line of nano-IR scanning points. We de-convoluted, i.e., statistically decompiled, the original non-normalized IR data into 6 Vectors, i.e., a combination of the 6 Vectors would result

in the original “convoluted” spectra; six Vectors provided sufficient statistical insight into the chemical bonding as a function of t_c .

Ballistics-Resistant Panels. The National Institute of Justice² defines panel failure as full perforation by projectile per minimum initial projectile velocity.³ Passing is quantified using 'back face signature,' or greatest extent of indentation in the backing material, caused by the non-perforating impact on armor. In our study, x -*IEPM*- b - t_c ballistics panels (thickness: 1.25 cm to 1.91 cm; 0.5 in to 0.75 in) were manufactured using 'hand lay-up' procedure. Each panel consisted of either four layers of *IEPM* or two layers of *IEPM* using combinations of t_c , polyurea type (aliphatic or aromatic), and epoxy-resin (low or medium viscosity). Each four-layer *IEPM* panel contained 20 layers of carbon fiber. Each panel was subjected to five calibers: .22LR (long rifle), 9mm Luger, .45Auto/ ACP, .357 Magnum, and .44 Magnum, Table S3. An additional two test programs (A and B for different epoxy-resin viscosity) were also used to check repeatability of results and to confirm correlation between lower t_c on nanostructures and ballistics resistance. Test program B used chronograph (RCBS AmmoMaster Chronograph®), placed at ten (10) feet from test panel, to measure the approach impact velocity of cartridges that were fired at twenty (20) feet. Our typical test set-up is shown in Figure S4.

Table S3. Five caliber-rated bullets used for ballistics-impact testing on x -*IEPM*- b - t_c

Ballistics Table Brand	Caliber	Bullet Weight (grain)	Bullet Type	Rated Muzzle Velocity (fps)	Rated Muzzle Energy (ft-lbs)
Federal	.22 LR	40	Lead round nose	1200	130
Remington UMC	9mm Luger	115	FMJ	1145	335
CCI Blazer	.45 Auto	230	FMJ	845	365
CCI Blazer Brass	.357 magnum	158	JHP	1250	548
Remington UMC	.44 magnum	180	JSP	1610	1036



Figure S4. Set-up of Test Program B, including wood-constructed support structure, chronograph, and *C-IEPM-b-t_c* test panel

1. Lee-Sullivan P, Dykeman D. Guidelines for performing storage modulus measurements using the TA Instruments DMA 2980 three-point bend mode: I. Amplitude effects1. *Polymer Testing*. **2000** Apr 1;19(2):155-64.
2. Armor PB. Ballistic Resistance of Personal Body Armor NIJ Standard–0101.04. **2008**
3. Abrate S. Impact on Composite Structures. *Cambridge university press*; **2005** Aug 22.